Modification of Shockley states induced by surface reconstruction in epitaxial Ag films on Cu(111)

A. Bendounan, H. Cercellier, Y. Fagot-Revurat, B. Kierren, V. Yu Yurov, and D. Malterre
Laboratoire de Physique des Matériaux, Université Henri Poincaré, Nancy I - Boîte Postale 239, F-54506 Vandœuvre-lès-Nancy, France
(Received 15 November 2002; published 16 April 2003)

Epitaxial Ag ultrathin films grown on Cu(111) have been studied by scanning tunneling microscopy and angle-resolved photoemission spectroscopy. In the submonolayer range, the spectroscopic measurements reveal the existence of two parabolic dispersive surface bands associated with the Cu terraces and the Ag islands suggesting the lateral confinement of the electronic states. A thickness dependence of the surface-state energy is evidenced. Moreover, the two well-known atomic reconstructions (moiré and triangular superstructures which depend on the preparation temperature) lead to different surface state energies. Photoemission spectra also reflect the transition from the metastable moiré structure into the triangular one. These results clearly demonstrate the strong sensitivity of the surface-state energy to the in-plane atomic structure.

DOI: 10.1103/PhysRevB.67.165412 PACS number(s): 73.20.At, 79.60.−i, 68.37.Ef

I. INTRODUCTION

Breakdown of periodicity occurring at single-crystal surfaces can lead to local modifications of the electronic properties. For the close-packed (111) surfaces of noble metals, new states are even induced known as Shockley states. These surface states develop in gaps of the bulk electronic structure and are characterized by a complex wave vector in the perpendicular direction. The imaginary part of the wave vector yields a damping of the wave function that only extends on few atomic layers. As a consequence, the surface states that only probe the vicinity of the surface, are very sensitive to its structural and chemical properties. Scanning tunneling microscopy (STM) and spectroscopy (STS) have revealed the modifications of surface states by step edges or nanoobjects such as islands or quantum corrals.[1–3]

Indeed, the sensitivity to adsorbed atoms was used to identify surface states or resonances and to separate them from the bulk states. As an example, it was often observed that adsorption of molecules, such as O_2 or CO, leads to the disappearance of surface states. However, inverse photoemission experiments showed that surface states sometimes do not actually disappear but are shifted above the Fermi Level. This is, for example, the case of O_2 on Cu(111) for which the surface-state energy at Γ was found about 3 eV above the Fermi level.[4] Recently, the modification of Shockley states by an adsorbed rare gas overlayer has been studied in details by STS and/or photoemission spectroscopy.[5–7] These spectroscopies showed that the surface-state energies are shifted above the Fermi energy. For example, in Xe/Ag(111), the minimum of the parabolic surface band is shifted from -60 meV for a clean Ag(111) surface to $+52$ meV for Ag(111) covered by one Xe monolayer (ML). In the case of Xe/Cu(111), the surface state remains in the occupied states but is significantly shifted toward the Fermi energy.[8]

Different situations can be encountered when atoms or molecules are deposited on a surface exhibiting a surface electronic state. If the overlayer is not ordered, the wave vector parallel to the surface is no longer conserved, and then the surface states are strongly broadened due to scattering by defects and even disappear. On the other hand, in the case of epitaxial overlayers, the lateral ordering is not destroyed and the surface state is preserved.[9] However, the surface potential and/or the work function are changed, leading to a shift of the surface-state energy.

Surface states are also sensitive to surface reconstructions. For instance, a (1×2) missing-row reconstruction is induced on Cu(110) by a room-temperature adsorption of a small amount of alkali metals, whereas no reconstruction is observed for deposition at low temperature. Photoemission and inverse photoemission spectra exhibit a very clear signature of the reconstructed surface.[10,11]

In the case of heteroepitaxial growth, many adatoms should occupy very unfavorable sites. As a consequence, surface reconstructions can be observed in order to release stress relaxation.[12–14] The Ag/Cu(111) interface can be considered as a model system in this problematic. Ag and Cu lattices are characterized by a 13% mismatch and these two elements are immiscible in the bulk. A (9×9) surface reconstruction was evidenced from low energy electron diffraction (Refs. 15 and 16) and has been interpreted by a quasicommensurate lattice since $d(\mathrm{Ag})/d(\mathrm{Cu})\simeq 9/8$. In fact, this interpretation is oversimplified and stress relaxation mechanisms, introduce important and complicated structural modifications that were shown with STM.[17,18] As discussed in this paper, this 9×9 reconstruction is induced by the formation of a lattice of dislocation loops in the substrate. This superstructure is only observed for films deposited at sufficiently high temperature (room temperature). For deposition at lower temperatures, the atomic structure is different and another superstructure without dislocation loops, is observed. Some spectroscopic studies of thin Ag films on Cu(111) have been already carried out. As the bulk gap of Ag(111) is smaller than the bulk gap of Cu(111), confinement of electronic waves in thin Ag layers is expected in the (111) direction. These quantum-well states have been intensively studied by angle-resolved photoemission spectroscopy (ARPES).[19] Nevertheless, a detailed ARPES investigation of the submonolayer range is still missing.

In this paper, we present an investigation of the surface electronic properties and their correlation with surface reconstructions in Ag ultrathin films deposited at different temperatures on a Cu(111) substrate. This manuscript is orga-

nized as follows. In Sec. II, we present the experimental details. Section III is devoted to the presentation and discussion of our experimental results : we first present the structural and electronic properties of room-temperature (RT) prepared films. We then compare with results obtained with films prepared at low temperatures (150 K). The different reconstructions corresponding to the two preparation temperatures are characterized by different surface states. We present the relation between structural and electronic changes at the transition from the moiré to the triangular structure. Finally, a numerical calculation to understand the surface energy modifications with thickness and elaboration temperature is presented.

II. EXPERIMENTAL DETAILS

The measurements were carried out in a UHV setup consisting in a molecular-beam epitaxy chamber for the elaboration and characterization of the surfaces, a STM chamber equipped with an Omicron STM1 operating at room temperature and a photoemission chamber with a high-resolution Scienta SES 200 analyzer. The photoemission experiments can be recorded between 20 K and room temperature. The He I radiation ($h\nu = 21.2$ eV) is provided by a high intensity UVS-300 SPECS discharge lamp operating at a pressure of 10^{-5} mbar in the ionization chamber. The energy resolution was better than 10 meV and angular resolution better than 0.5°. The electrons are collected by a microchannel plate and accelerated onto a phosphorus screen monitored by a charge-coupled device (CCD) camera. This two-dimensional (2D) detector allows to record accurately the emission spectra between -8 and $+8$ degrees without rotating the sample. The Cu substrate was first prepared by a mechanical polishing followed by 5 mn of an electrochemical polishing in an orthophosphoric acid solution. After introduction in the UHV setup, the substrate was cleaned by several cycles of Ar^+ sputtering at 2000 eV and annealing at 600 °C . The morphology of the sample was characterized by scanning tunnelling microscopy. Due to an uncontrolled miscut with respect to the (111) planes, a rather high density of steps was observed on this sample. The cleanness was checked using STM and a Ribber cylindrical mirror analyzer for auger electron spectroscopy. The Ag atoms were evaporated from a Knudsen cell operating at $T = 950$ °C at a rate in the range of 0.5–2 ML/mn. This rate was measured by monitoring the frequency shift of a quartz microbalance with a 12 digits counter. The calibration was achieved by STM measurements which were in agreement with the photoemission and AES data (see Sec. III A). During Ag deposition, the substrate temperature could be adjusted between RT and 100 K.

III. RESULTS AND DISCUSSION

A. Growth and electronic properties of Ag/Cu(111) at room temperature

We have studied Ag ultrathin films deposited on Cu(111) by STM and ARPES. In Figs. 1(a) and 1(b), we present STM images of 0.4 ML and 1.2 ML Ag films, respectively, prepared at room temperature. As previously described in

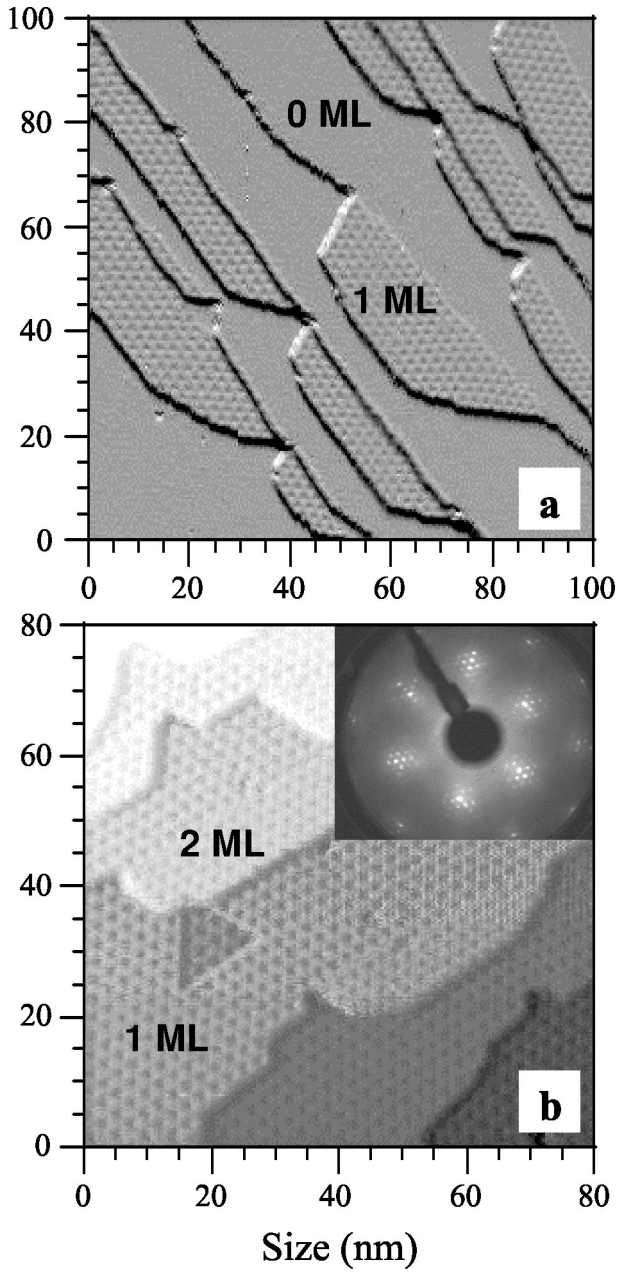

FIG. 1. STM images corresponding to the 0.4 ML (a) and 1.2 ML (b) Ag films. Insert: LEED pattern of the 1.2 ML film.

literature,[17,9,20] the 0.4 ML image shows that all epitaxial Ag islands are of monoatomic height and are connected to the ''downhill'' side of the substrate step edges. This means that for submonolayer films, the Cu step edges are the nucleation sites for Ag island growth and that, at room temperature, the diffusion length of the Ag adatoms on Cu(111) is at least several hundred angstroms. For the 1.2 ML film, Ag islands grew after the first Ag layer was completed and they are also connected to step edges. A large scale modulation is clearly visible on the Ag islands and is associated with the 9×9 superstructure evidenced in LEED experiments [inset of Fig. 1(b)]. A layer-by-layer growth was proposed for Ag epitaxy at room temperature.[21] This is in agreement with our STM observations and the evolution of the photoemission Ag 4*d*

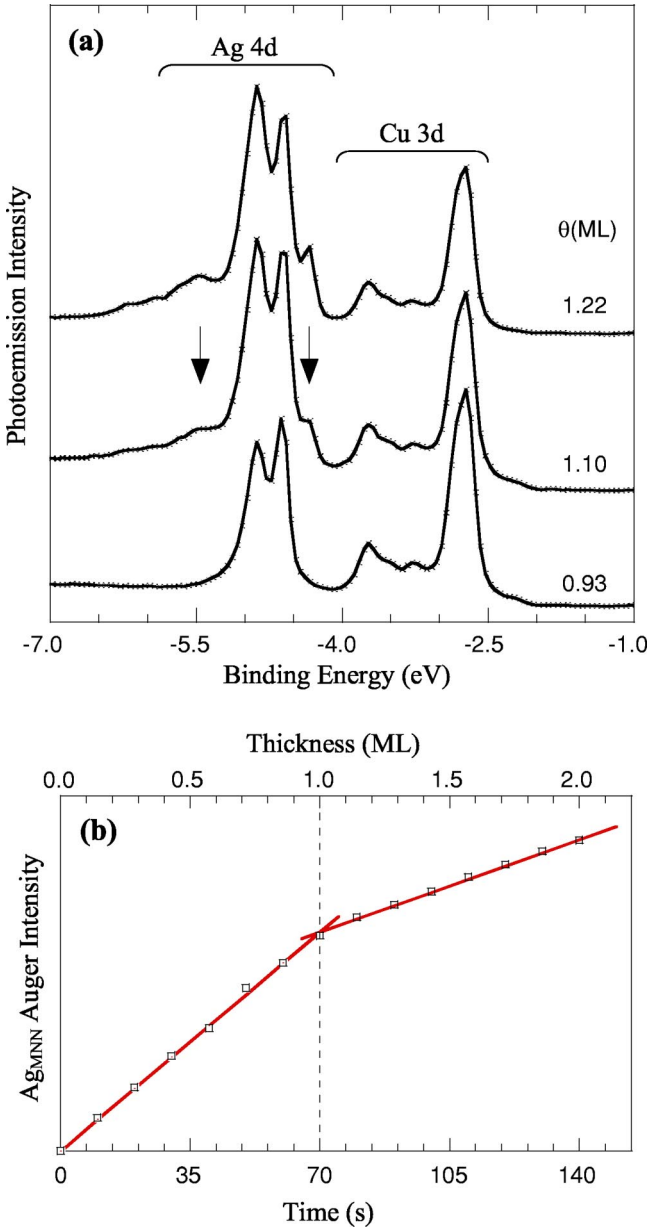

FIG. 2. (a) Photoemission valence-band spectra for several Ag coverage, the arrows indicate the appearance of the spectral features associated with the second Ag layer. (b) Ag Auger intensity as function of time (or coverage).

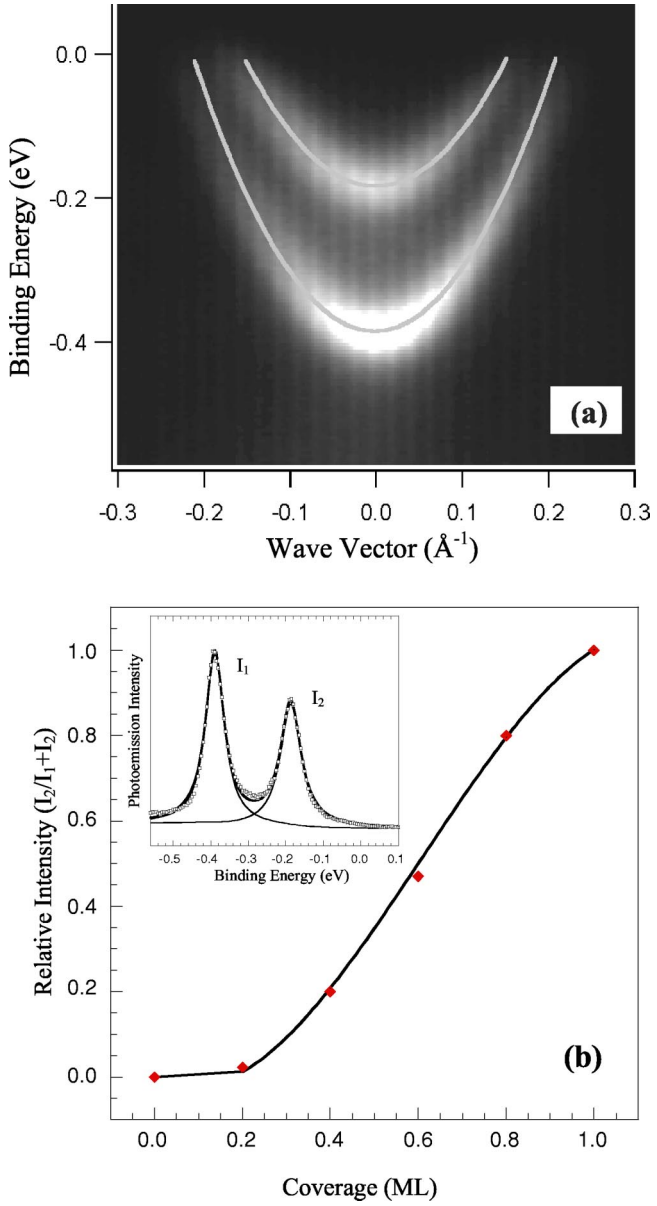

FIG. 3. (a) Room temperature photoemission map (intensity in gray scale as function of energy and wave vector) for a 0.6-ML Ag film. The solid lines represent a fit corresponding to a quadratic dispersion $E(k)=\hbar^2k^2/2m^\star+E_0$, (b) relative intensity of the two spectral features in the normal emission spectra as function of Ag coverage (the solid line is a guide for the eye). Intensities I_1 and I_2 are obtained by fitting the normal emission spectra with two lorentzians as shown in the inset.

bands. In the submonolayer range, the *d* bands consist of two narrow peaks. A sudden change of the shape [additional structures indicated by arrows in Fig. 2(a)] is observed at the completion of the first Ag monolayer. This is corroborated by the change of the slope in the Ag AES signal [Fig. 2(b)]. For larger coverage ($\theta>2$ ML), a tridimensional growth was observed in agreement with published data.[17]

STS measurements, we published in previous papers,[9,20] showed that confinement of surface states occurs. In submonolayer Ag films, two kinds of differential conductivity spectra were obtained on Cu terraces and Ag islands. The two spectral features separated by 220 meV suggest that two surface states coexist in this system, one confined in Cu terraces and the other one in Ag islands. Photoemission spectroscopy corroborates these results and shows that two electronic states exhibit a parabolic dispersion characteristic of the nearly free electron nature of the Cu(111) surface state [Fig. 3(a)].

The energy difference (200 meV) measured on the normal emission spectrum [inset of Fig. 3(b)] corresponding to the $\overline{\Gamma}$ point of the surface Brillouin zone, is in agreement with the previous STS results (220 meV) and can be interpreted by the modification of the potential probed by surface electrons (cf Sec. III D). Indeed, surface states are confined in the nor-

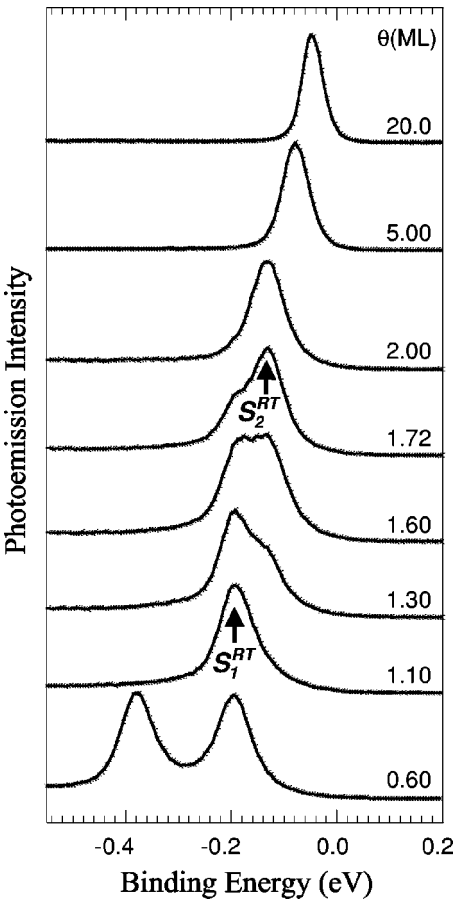

FIG. 4. Normal emission spectra for several Ag coverage, S_1^{RT} and S_2^{RT} indicate the spectral features associated with 1-ML- and 2-ML-thick Ag films.

mal direction in the quantum well consisting of the vacuum level on one side and the bulk gap on the other side.[22] By depositing one Ag monolayer on Cu(111), the quantum well potential is modified and the energy of Cu(111) surface state is changed. The presence of two well-defined surface-state energies in normal emission spectra of submonolayer films suggests that the surface electrons probe either the bare Cu(111) potential or a Cu potential modified by the Ag layer. The system can be described by two kinds of wave functions, one associated with free Cu areas and the other one with the Ag covered areas. This behavior is in complete agreement with the STS results and confirms the lateral confinement of the surface states in Cu terraces and Ag islands. Therefore, with increasing Ag coverage from 0 to 1 ML, a balance of spectral weight between the two structures associated with Cu terraces and Ag islands is observed [Fig. 3(b)] in agreement with the assumption that they are associated with the two kinds of surface terminations. With increasing θ, the Ag island contribution has to increase whereas the Cu one has to decrease. A similar behavior is observed in the 1–2 ML range. Two normal emission features are observed exhibiting the same balance of spectral weight as function of Ag coverage (Fig. 4). The S_1^{RT} structure ($E_B=-190$ meV) corresponds to the 1-ML Ag film, whereas the S_2^{RT} one ($E_B=-130$ meV) is the signature of the second Ag layer. For larger film thicknesses, only one spectral feature is exhibited with a progressive shift toward the position of the surface state of Ag(111) in Ag single crystal ($E_B=-45$ meV at room temperature). Two arguments can be invoked to explain the observation of only one spectral feature for $\theta>2$ ML. First, the energy difference between surface states corresponding to n and $(n+1)$ Ag layers decreases as the number of Ag overlayers increases, so that the two surface states are less and less resolved. Second, a tridimensional growth is encountered above 2 ML and the spectral feature is composed of several unresolved contributions. One has to note that the energy of the S_1^{RT} and S_2^{RT} structures does not significantly depend on the coverage (Fig. 4). This is due to the large size of Ag islands resulting from the growth mechanism and to the large mobility of Ag adatoms on the Cu(111) substrate. Indeed quantum size effect associated with the lateral confinement of electronic states in islands should be expected. In a simple quantum-well approach, the energy shift due to confinement is inversely proportional to the square of the lateral size leading to a vanishing effect for large islands. For islands larger than 10 nm, the energy shift can be estimated to be smaller than 5 meV, that was experimentally verified.[2] To evidence a sizeable energy shift with photoemission, very small islands (<10 nm) with sharp size distribution are necessary. To investigate this point, Ag deposition at low temperature (150 K) has been carried out. With decreasing deposition temperature, a decrease in the Ag adatom mobility is expected leading to Ag islands smaller than for room temperature deposition.

B. Electronic states in the $T=150$ K prepared films

We deposited Ag films at low temperature (150 K) and measured them at room temperature, in order to compare with STM measurements. The normal emission spectra for several Ag coverage reveals a systematic evolution (Fig. 5).

In the submonolayer range ($\theta<1$ ML), two spectral features at $E_B=-390$ meV and $E_B=-290$ meV (S_1^{LT}) are observed. The intensity of the peak at $E_B=-390$ meV decreases with increasing Ag coverage and vanishes for $\theta=1$ ML. It corresponds to the surface state confined in the Cu terraces. The S_1^{LT} structure intensity increases with Ag coverage and then can be identify to the electronic state confined in the Ag islands like for the room temperature experiments. The energy of this spectral feature is Ag coverage independent suggesting that Ag islands are still too large to modify the energy of the confined electronic states. In the 1 ML$<\theta<2$ ML thickness range, two structures at $E_B=-290$ meV (S_1^{LT}) and $E_B=-170$ meV (S_2^{LT}) are also observed and correspond to surface states associated with regions with different Ag film thicknesses (1 ML and 2 ML). Comparison with the data obtained on films deposited at room temperature shows that the structure associated with Cu terraces appears at the same energy ($E_B=-390$ meV), whereas the structures associated with 1-ML-thick (S_1^{LT}) and 2-ML-thick (S_2^{LT}) Ag films are shifted to higher binding energy by $\Delta E_1=100$ meV and $\Delta E_2=40$ meV, respectively (Table I).

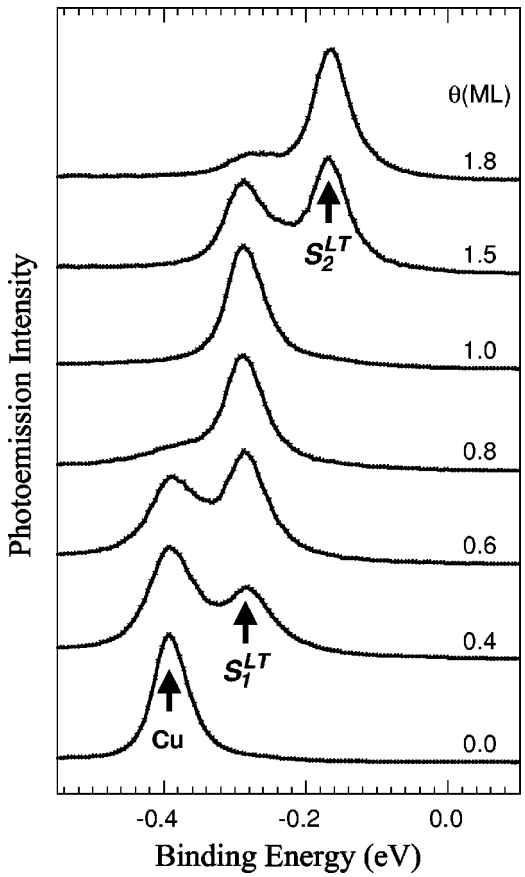

FIG. 5. Normal emission spectra for several films prepared at $T=150$ K.

In order to understand this difference, a soft annealing of the films has been achieved. Figure 6 illustrates the effect of an annealing at 400 K.

In the submonolayer range, an irreversible spectral modification is observed for the Ag related structure. The normal emission structure (S_1^{LT}) is shifted by about 100 meV towards the Fermi energy (S_1^{ann}). The energy value measured on a room temperature deposited film (S_1^{RT}) is restored, so that in the 0–1 ML range the spectra of the annealed films are very similar to the spectra of room temperature prepared films. On the contrary, in the 1 ML$<\theta<$2 ML range, after annealing, the surface-state energy associated with the second Ag monolayer feature (S_2^{ann} with $E_B=-160$ meV) does not correspond to the energy measured on the room temperature prepared films ($E_B=-130$ meV). This is illustrated in Fig. 7 that presents the annealing effect on a 1.6-ML film. The two images in Fig. 7(a) represent the photoemission intensity as function of energy and wave vector for a T

TABLE I. Values of $\bar{\Gamma}$ energy for the surface states observed on films prepared at room temperature, at 150 K and after an annealing (see text).

E	Cu	S_1^{RT}	S_2^{RT}	S_1^{LT}	S_2^{LT}	S_1^{ann}	S_2^{ann}
E_0 (meV)	−390	−190	−130	−290	−170	−190	−160

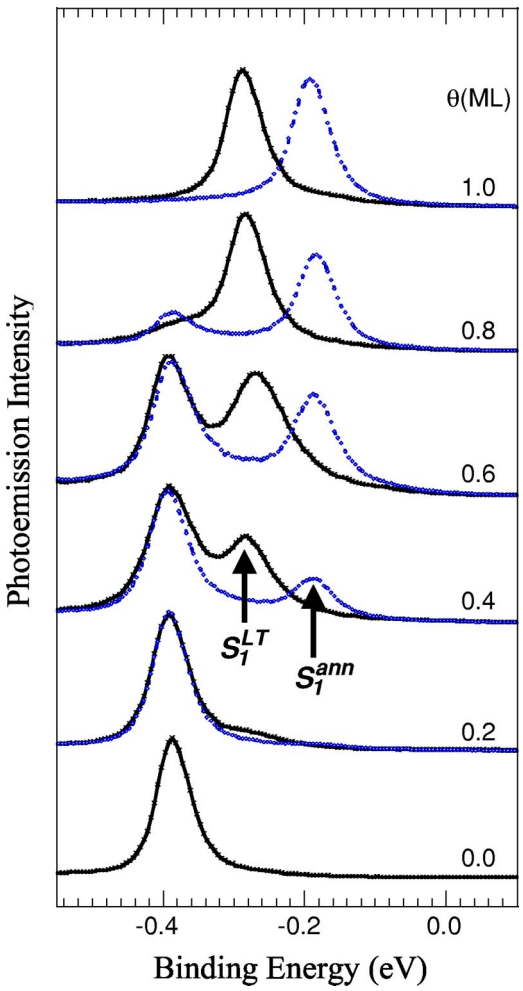

FIG. 6. Normal emission spectra for several Ag submonolayers prepared at $T=150$ K (solid lines) and after annealing at $T=400$ K (dotted lines).

$=150$ K prepared film and after an annealing at $T=400$ K. The spectra of the $T=150$ K deposited film exhibit two parabolic dispersive bands, whereas only one band is evidenced for the annealed film. Analysis of the normal emission spectra [Fig. 7(b)] shows that for the room temperature prepared film, the two bands are separated by 60 meV at the $\bar{\Gamma}$ point, whereas only one spectral line close to $E_B=-180$ meV appears for the annealed film. This single line is in fact composed of two unresolved contributions, one (S_1^{ann}) at $E_B=-190$ meV corresponding to regions covered by one monolayer and the other one, corresponding to the second monolayer (S_2^{ann}), at $E_B=-160$ meV; this latter value being very close to the low temperature one $E_B=-170$ meV. This suggests that the atomic structure of the second monolayer regions are only weakly affected by the annealing. A comparison with the spectrum obtained on a 1.6 ML film deposited at room temperature [upper curve in Fig. 7(b)] clearly shows that the spectra associated with 1-ML-thick regions of the room temperature prepared and annealed films are very similar, whereas significant differences exist for regions covered by two monolayers.

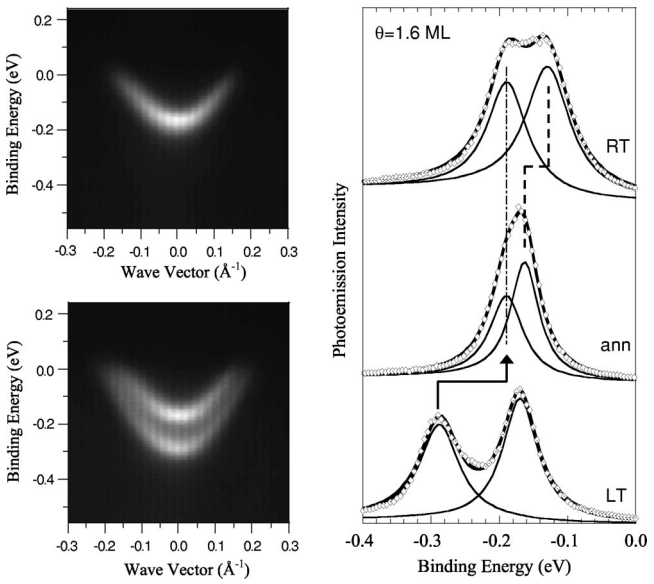

FIG. 7. (a) Room temperature photoemission map (intensity in gray scale as function of energy and wave vector) for a 1.6-ML film prepared at $T=150$ K (bottom image) and after annealing at $T=400$ K (top image); (b) normal emission spectra corresponding to the film prepared at 150 K (LT) and after annealing (ann). For comparison, the normal emission spectrum of the room temperature prepared film (RT) is also reported.

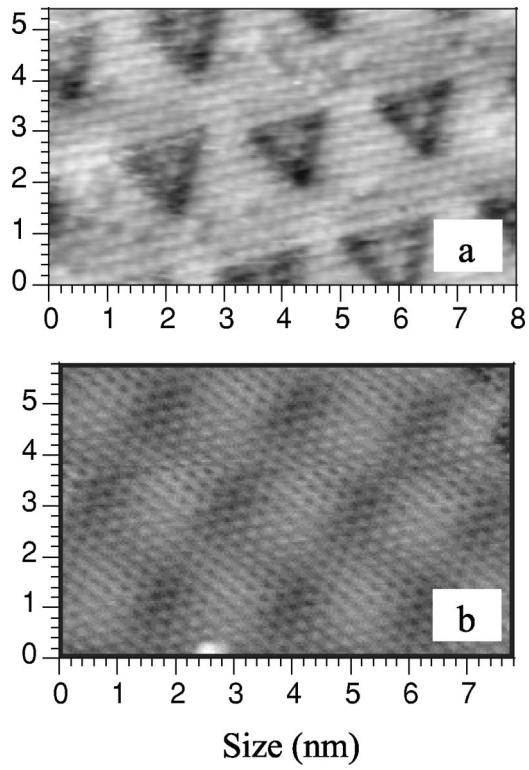

FIG. 8. STM images of 1-ML-thick Ag film elaborated at room temperature (a) and at $T=150$ K (b).

These irreversible modifications of photoemission spectra observed after the $T=400$ K annealing can be explained by a change of the surface atomic structure. To illustrate this point, STM has been carried out on low and room temperature prepared films. Figure 8 shows atomic scale images obtained on Ag islands corresponding to room temperature (a) and $T=150$ K (b) prepared films. For the RT elaborated or annealed films, the well-known triangular superstructure is observed. STM images evidenced two kinds of triangles with three or six atoms protruding in the center.

Sometimes, we also observed triangles with only one atom in the center. This is in agreement with previous investigations reported for this system.[18] The quasi (9×9)-superstructure, evidenced by LEED (Ref. 15) and recent x-ray surface diffraction experiments,[23] arises from the periodic arrangement of these triangles. The black part of the triangles has not to be interpreted as missing atoms in the first Ag layer since calculations indicate that such a configuration is very unstable. As for Au/Ni(111),[24] the triangular corrugation arises from the formation of dislocation loops in the top layer of the substrate with a removal of some Cu atoms. Such a mechanism is associated with the shift of several Cu atoms from fcc to hcp sites. This interpretation has been recently supported by quantum molecular dynamics simulations.[25] These calculations show that the reconstruction of the top substrate layer occurs by the introduction of a few vacancies collapsing in a partial dislocation loop. This mechanism leads to a morphology that is in almost perfect agreement with STM images[25] and with impact collision ion-scattering spectroscopy.[26]

The atomic structure of the films deposited at low temperature is different. Diffraction patterns also exhibit a 9 $\times$9 superstructure, but STM shows that the atomic structure [Fig. 8(b)] consists of the superposition of the hexagonal closed-packed symmetry of Cu and Ag layers yielding a moiré structure. This is very similar to the structure of Au overlayers on Ni(111) deposited at low temperature.[24] In this atomic arrangement, many atoms occupy poorly favorable position with respect to the substrate (Ag atoms on top on Cu atoms). For this reason, the moiré structure is unstable and relaxation processes yield the triangular structure that is more stable. It is natural to ascribe the change in the photoemission spectra as mainly due to the modification of the atomic reconstruction which depends on the preparation temperature. This dependence reflects the modification of the potential probed by surface electrons as we will discuss in Sec. III D.

C. Transition from the moiré to the triangular structure

Unfortunately the moiré structure is not stable enough and its study with a room temperature STM is quite difficult. At this temperature, a time evolution can be evidenced due to a progressive transformation from the moiré to the triangular structure. This is shown in Fig. 9, where we present a STM image recorded after the room temperature thermalization of the sample.

On the left picture, a large Ag island appears on a Cu(111) terrace. As the tunneling current has been recorded with a closed feedback loop (constant current mode), only the highest spatial frequencies are visible, leading the same average gray tone for the Ag island and the neighboring Cu terrace. However, if the moiré superstructure exists on the main part

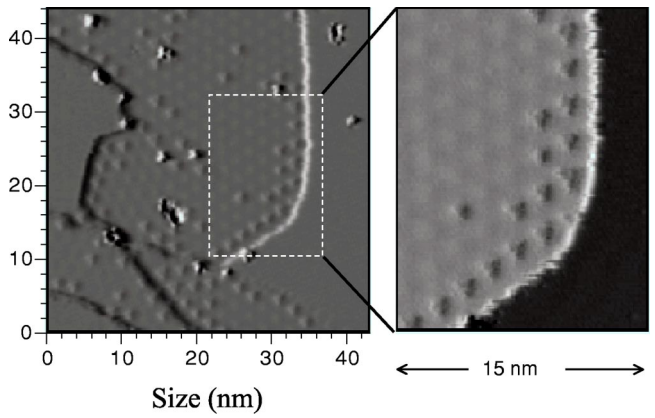

FIG. 9. STM images recorded in constant current mode on a 0.6-ML Ag film prepared at $T=150$ K. Left: tunneling current; right: topographic signal. Some triangular features, precursors of the moiré-triangular transition, appear near the Ag island edge.

of the island (close up in Fig. 9), one can distinguish some triangles close to the island boundaries. This observation results from the irreversible transformation of the moiré structure into the triangular one. Several images recorded on the same area as function of time reveal the progressive transition at room temperature by the appearance of new triangles. Figure 10 exhibits the spectroscopic consequence of this transition. The time dependence of normal emission spectra is reported for a 0.6-ML film. The Ag film was prepared at low temperature ($T=150$ K) and measured at room temperature as function of time. Just after preparation, the normal emission spectrum (a) exhibits two features at $E_B=-390$ meV, reflecting the Cu terrace contribution, and at $E_B=-290$ meV corresponding to Ag islands (structure labeled A or S_1^{LT} in the previous discussion) that all exhibit the moiré superstructure. After an annealing at 400 K, the island related feature is shifted to $E_B=-190$ meV (structure labeled C or S_1^{ann}) as shown on the top curve of Fig. 10. This latter spectral feature corresponds to the triangular superstructure also observed for room temperature prepared films (S_1^{RT}).

In between, a continuous evolution of the surface states is observed. After 1 h at room temperature, a shoulder has appeared at $E_B=-250$ meV (structure labeled B in Fig. 10). After 3 h, the spectra are then a mixture of the three (A, B, and C) contributions as shown in spectrum (c) of Fig. 10. This observation suggests a transient atomic structure. The STM image shown in Fig. 11, recorded after the first photoemission measurements spectrum (a), corroborates this interpretation. Most part of this image reveals the atomically resolved moiré structure. However several large (about 1.5 nm) dark regions also appear. In contrast to the triangular structure observed on room temperature prepared films for which some atoms are clearly observed in the center, no atoms are resolved in these dark areas. It is natural to ascribe the B peak in the photoemission spectra as an electronic signature of this new structure. Thus, the transition from the moiré to the triangular structure takes place through an intermediate state, characterized by a specific atomic structure with its own spectroscopic signature. These results shed light on the

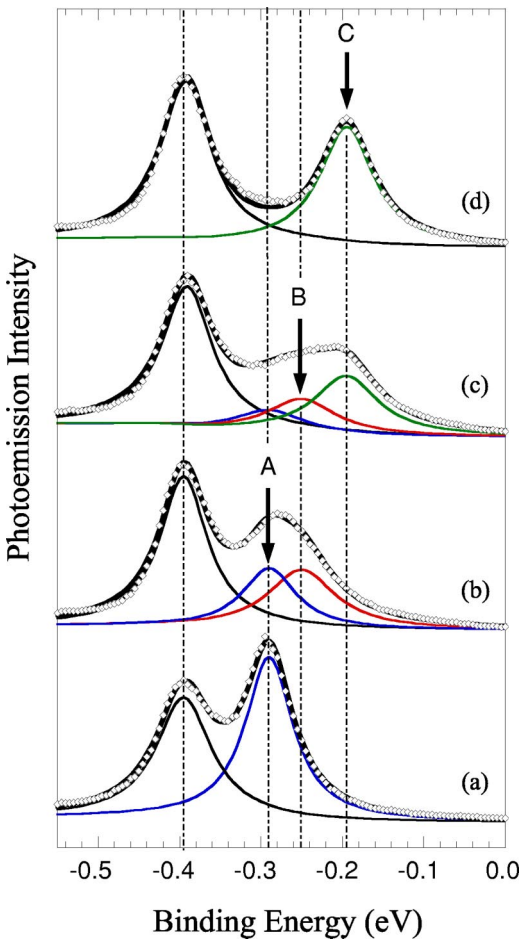

FIG. 10. Photoemission measurements revealing the irreversible transition from the moiré to the triangular superstructure : (a) $T=300$ K just after deposition, (b) $T=300$ K, 1 h later, (c) $T=300$ K, 3 h later, and (d) after an annealing at $T=400$ K. A, B, and C represent the spectral features associated with the moiré, the intermediate, and the triangular structures, respectively.

extreme sensitivity of surface states to structural modifications at the surface, especially in the case of strong local atomic reconstructions (at the nanoscopic scale).

The position in energy of the surface states depends on the film thickness and on the atomic reconstruction of the interface corresponding to the preparation temperature. From the values tabulated in Table I, the effect of annealing on the reconstruction can be deduced. For 1-ML-thick Ag island, the surface-state energy associated with the triangular structure is restored corroborating the STM results which exhibit a transformation from the moiré to the triangular structure. This transformation corresponds to the formation of dislocation loops in the Cu substrate. Then for such islands, there is no difference between films prepared at room temperature and films prepared at $T=150$ K and further annealing. For 2-ML-thick Ag layers, there is negligible effect of annealing on the surface-state energy. This result suggests that the moiré-triangular transformation does not occur. These results are schematically summarized in Fig. 12. We can suggest that the 2-ML Ag film is too thick and prevents the expulsion of Cu atoms necessary for the formation of the dislocation

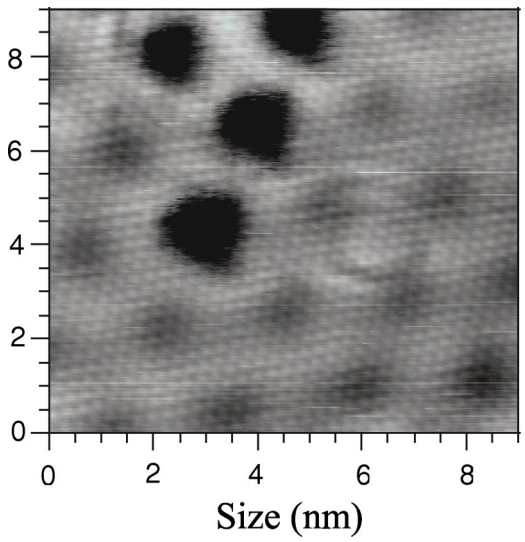

FIG. 11. STM image revealing the existence of an intermediate structure (dark regions); the atoms clearly visible in the room temperature triangular structure are not resolved.

loops. This is corroborated by the observation, in the first stage of the moiré-triangular transition, of triangles close to the islands boundaries (Fig. 9): vacancy mobility and relaxation should be favored near island edges.

D. Calculation of the surface-state energy

The above measurements show the interplay between atomic structure and electronic properties of the surface. A simple approach can reproduce the experimental energy of the surface states. As discussed above, the growth mechanism leads to large Ag islands connected on step edges of the Cu substrate. Despite the fact that the surface states are confined in the Ag islands, no sizeable energy shift is observed due to the large size of the islands. As a consequence, the lateral dimension of the islands is not a pertinent parameter and a one-dimensional approach should be sufficient to explain the shift of the surface-state energy. As mentioned in the Introduction, the Shockley surface state of Cu(111) develops close to the L point in a gap of the bulk band structure. A framework based on a pseudopotential with only one Fourier component (V_G), associated with the corresponding reciprocal vector, provides a simple approach to obtain the bulk band structure with a gap of magnitude $2V_G$ at the limit of the Brillouin zone. The surface state corresponds to a perpendicular complex wave vector for an energy level in the gap. The energy value is obtained by considering the potential outside the crystal, and the condition of continuity of the wave function and its derivative. We have chosen the surface potential, recently proposed by Chulkov *et al.*[27–29] We essentially adjust the β factor (as defined in Ref. 27) to reproduce the surface-state energy we obtained at room temperature for Cu(111) ($E_B=-390$ meV) and for Ag(111) ($E_B=-45$ meV). Calculations have been carried out for integer numbers of Ag layers. The potential in the vacuum region (image potential) is kept constant with Ag film thickness. The wave function is obtained from a numerical calculation

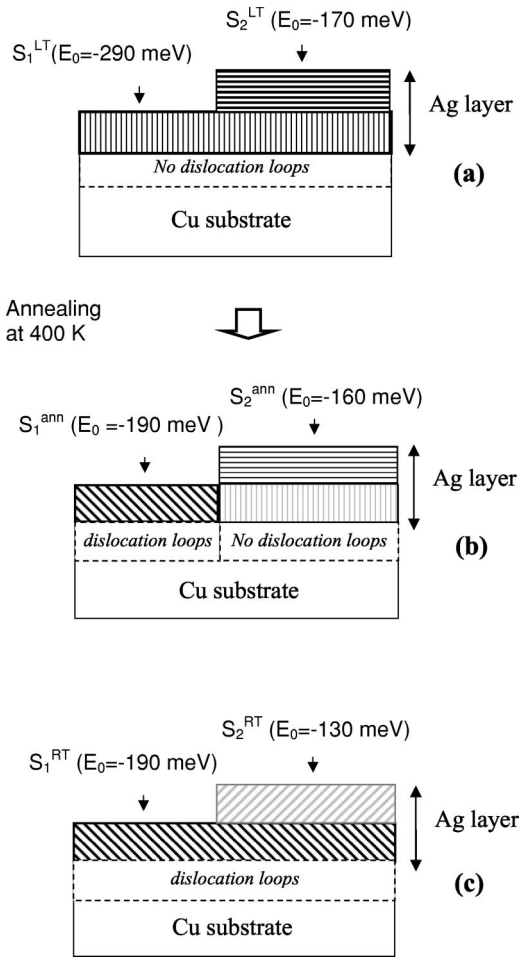

FIG. 12. Schematic view of the room temperature structure for 1-ML and 2-ML Ag films on Cu(111) deposited at room temperature (c), deposited at 150 K (a) and deposited at 150 K and after an annealing at 400 K (b).

(Numerov algorithm[30]). By averaging the potential in the planes parallel to the (111) surface, one obtains a one-dimensional Schrödinger equation,

$$\frac{d^2\Psi(z)}{dz^2}=-\frac{2m}{\hbar^2}[E-V(z)]\Psi(x)=f_E(z)\Psi(z),$$

where V(z) is the spatial dependence of the average electron potential in the normal direction [V(z) depends on the in-plane structure]. Its solution gives the $\vec{k}_{\parallel}=0$ surface-state energy. The Numerov algorythm is based on second-order Taylor development of the one-dimensional Schrödinger equation,

$$\Psi(z\pm\varepsilon)=\Psi(z)\pm\varepsilon\frac{d\psi}{dz}+\frac{\varepsilon^2}{2}\frac{d^2\psi}{dz^2}+O(\varepsilon^3).$$

A fourth-order development of the second derivative in the

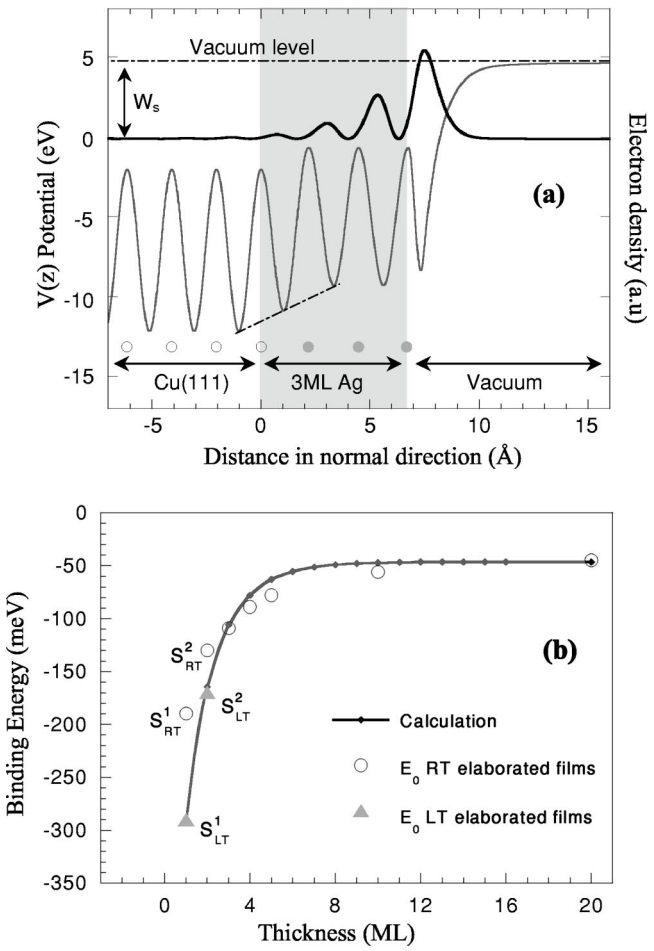

FIG. 13. (a) Illustration of the calculation of the surface-state energy, for a 3-ML Ag film on Cu(111). The thick solid line (upper curve) represents the electron density of the surface state and the thin solid line represents the potential in the Cu substrate, the Ag layer and the vacuum. The open symbols represent the Cu planes, whereas the black ones represent Ag planes. (b) Comparison of the calculated and experimental values of the surface-state energy for 0 ML$<\theta<$20 ML.

Schrödinger equation allows to obtain a recurrence relation for the wave function :

$$\Psi(z+\varepsilon) = \frac{\Psi(z)\left[2+\frac{5\varepsilon^2}{6}f_E(z)\right]+\Psi(z-\varepsilon)\left[\frac{\varepsilon^2}{12}f_E(z-\varepsilon)-1\right]}{\left[1-\frac{\varepsilon^2}{12}f_E(z+\varepsilon)\right]}.$$

As a consequence, the knowledge of the wave function at two neighboring points $[\Psi(z-\varepsilon)$ and $\Psi(z)]$ gives the wave function at the following point $[\Psi(z+\varepsilon)]$. A convergent solution at large z is only obtained for the values of energy corresponding to the genuine eigenvalues (surface-state energies). In Fig. 13, we show the $V(z)$ potential of a 3-ML Ag film. It consists of three regions : first, the one-dimensional periodic potential corresponding to the Cu region; second, three periods corresponding to the three Ag layers; and finally, the image state potential in the vacuum. To describe the potential at the interface, a linear dependence in the first Ag plane between the Cu and Ag inner potentials is used as can be shown on the dashed segment in Fig. 13.

It is clear from this picture that for Ag thickness larger than the attenuation length of the surface-state (about 5 atomic layers), the surface state energy should tend to the value obtained at room temperature in pure Ag(111) ($E_B=-45$ meV). In Fig. 13(b), we show the experimental thickness dependence of the surface-state energy compared to the calculated ones. A good agreement is observed at least for films deposited at low temperature. The deviation from the layer-by-layer growth for $\theta>2$ ML can explain the small difference observed. We would like to point out that the calculation does not account the surface-state energy for 1-ML-thick films prepared at room temperature. This corroborates the fact that in these latter films, strong relaxation processes (dislocation loops) affecting several Cu layers occur. These mechanisms should strongly modify the potential. On the contrary, the moiré structure that is simply a superposition of Cu and Ag layer is correctly described in our calculations that assume a similar superposition of Cu and Ag potentials.

IV. CONCLUSION

In this paper, we have studied the evolution of the surface state of Ag ultrathin films on Cu(111). We have shown that the modification of the surface-state energy reflects the morphology and the atomic structure of the surface. For submonolayer films deposited at room temperature, large Ag islands are found to be connected to the substrate step edges. STS and ARPES results indicate the presence of two surface states, laterally confined in the Ag islands and Cu terraces. Moreover, a shift of the surface state with respect to the Cu(111) surface reflects the formation of a 9×9 superstructure induced by strong relaxation processes in the Cu top layer (triangular structure). Low temperature deposited films exhibit a different surface-state energy associated with Ag islands. This difference results from a different atomic structure, since a metastable moiré structure is formed at low temperatures. The irreversible transition between these two structures has been also studied by photoemission spectroscopy; a spectral signature associated with a transient structure has been identified. All these measurements emphasize the strong interplay between electronic and structural properties in this system due to the great sensitivity of surface-state energy to the surface and interface reconstructions. In addition, we have shown that probing Shockley states with high resolution photoemission spectroscopy can give reliable information not only on the surface but also on the interface structure.

ACKNOWLEDGMENTS

We would like to acknowledge E. Moyen and L. Piot for their contributions to the numerical simulations presented in this paper.

[1] M.F. Crommie, C.D. Luz, and D.M. Eigler, Nature (London) **363**, 524 (1993).
[2] J. Li, W.-D. Schneider, S. Crampin, and R. Berndt, Surf. Sci. **422**, 95 (1999).
[3] L. Bürgi, H. Brune, O. Jeandupeux, and K. Kern, J. Electron Spectrosc. Relat. Phenom. **109**, 33 (2000).
[4] C.T. Chen and N.V. Smith, Phys. Rev. B **40**, 7487 (1989).
[5] H. Hövel, B. Grimm, and B. Reihl, Surf. Sci. **477**, 43 (2001).
[6] R. Paniago, R. Matzdorf, G. Meister, and A. Goldmann, Surf. Sci. **325**, 336 (1995).
[7] J.-Y. Park, S.-J. Kahng, U.D. Ham, Y. Kuk, K. Miyake, K. Hata, and H. Shigekawa, Phys. Rev. B **60**, 16 934 (1999).
[8] F. Forster, G. Nicolay, F. Reinert, D. Ehm, S. Schmidt, and S. Hüfner, Surf. Sci. (to be published).
[9] A. Bendounan, Y. Fagot-Revurat, B. Kierren, F. Bertran, V. Yu Yurov, and D. Malterre, Surf. Sci. **496**, L43 (2002).
[10] P. Sandl and E. Bertel, Surf. Sci. **302**, L325 (1994).
[11] N. Memmel, Surf. Sci. Rep. **32**, 91 (1998).
[12] J.W. Matthews, in *Epitaxial Growth*, edited by J.W. Matthews (Academic, New York, 1975), pt. 1, p. 559.
[13] J.H. van der Merwe, in *Chemistry and Physics of Solid Surfaces*, edited by R. Vanselow and R. Howe (Springer, Berlin, 1984), p. 365.
[14] J.H. van der Merwe, D.L. Tönsing, and P.M. Stoop, Surf. Sci. **312**, 387 (1994).
[15] K.A.R. Mitchell, D.P. Woodruff, and G.W. Vernon, Surf. Sci. **46**, 418 (1974).
[16] E. Bauer, Appl. Surf. Sci. **11-12**, 479 (1982).
[17] W.E. McMahon, E.S. Hirschorn, and T.-C. Chiang, Surf. Sci. **279**, L231 (1992).
[18] F. Besenbacher, L. Pleth Nielsen, and P.T. Sprunger, in *Chemical Physics of Solid Surfaces and Heterogeneous Catalysis*, edited by D.A. King and D.P. Woodruff (Elsevier Science, Amsterdam, 1997), Vol. 8, Chap. 10.
[19] T.-C. Chiang, Surf. Sci. Rep. **39**, 181 (2000)
[20] V.Yu. Yurov, A. Bendounan, B. Kierren, Y. Fagot Revurat, F. Bertran, and D. Malterre, Phys. Low-Dimens. Struct. **11-12**, 155 (2001).
[21] Y. Borensztein, Europhys. Lett. **4**, 723 (1987).
[22] N.V. Smith, Phys. Rev. B **32**, 3549 (1985)
[23] B. Aufray, M. Göthelid, J-M. Gay, C. Mottet, E. Landemark, G. Falkenberg, L. Lottermoser, L. Seehofer, and R.L. Johnson, Microsc. Microanal. Microstruct. **8**, 167 (1997).
[24] J. Jacobsen, L. Pleth Nielsen, F. Besenbacher, I. Stensgaard, E. Laegsgaard, T. Rasmussen, K.W. Jacobsen, and J.K. Norskov, Phys. Rev. Lett. **75**, 489 (1995).
[25] I. Meunier, G. Tréglia, J.-M. Gay, B. Aufray, and B. Legrand, Phys. Rev. B **59**, 10 910 (1999).
[26] K. Umezawa, S. Nakanishi, M. Yoshimura, K. Ojima, K. Ueda, and W.M. Gibson, Phys. Rev. B **63**, 035402 (2001).
[27] E.V. Chulkov, V.M. Silkin, and P.M. Echenique, Surf. Sci. **391**, L1217 (1997).
[28] E.V. Chulkov, V.M. Silkin, and P.M. Echenique, Surf. Sci. **437**, 330 (1999).
[29] P.M. Echenique, J.M. Pitarke, E.V. Chulkov, and A. Rubio, Chem. Phys. **251**, 1 (2000).
[30] B. Numerov, Publ. Obs. Central Astrophys. **2**, 188 (1933).